Countermeasures of Zero-missing Phenomenon in (E)HV Cable Systems

Khalilnezhad, Hossein; Popov, Marjan; van der Sluis, Lou; Bos, Jorrit A.; de Jong, Jan P.W.; Ametani, Akihiro

DOI
10.1109/TPWRD.2017.2729883

Publication date
2018

Document Version
Final published version

Published in
IEEE Transactions on Power Delivery

Countermeasures of Zero-Missing Phenomenon in (E)HV Cable Systems

Hossein Khalilnezhad, *Graduate Student Member, IEEE*, Marjan Popov, *Senior Member, IEEE*, Lou van der Sluis, *Life Senior Member, IEEE*, Jorrit A. Bos, Jan P. W. de Jong, and Akihiro Ametani, *Life Fellow, IEEE*

***Abstract*—Zero-missing is a phenomenon in shunt-compensated cable systems, in which the current through the line breaker does not cross the zero point for several cycles. This paper deals with a thorough investigation on countermeasures of the zero-missing phenomenon in transmission systems and determines the requirements, benefits, and risks of applying each method. The effectiveness of countermeasures is studied on a simulated cable project with different cable lengths in an actual grid model of the Dutch 380 kV transmission system. Results are analyzed based on three criteria related to the IEC standards and the Dutch grid code. In addition, the switching sequence of circuit breakers is specified to maximize the effectiveness of the countermeasures. A statistical switching analysis is performed for the insulation coordination study since the application of some countermeasures increases the probability of high transient switching overvoltages. Moreover, the closing variation threshold of circuit breakers is calculated as a function of the circuit impedance and the shunt compensation degree.**

***Index Terms*—Cables, circuit breakers, shunt reactor, switching transients, statistical analysis, zero-missing phenomenon.**

I. Introduction

THE application of long (E)HV AC cables in future transmission grid expansions is under the study or has already been planned by many system operators. The operation of long cables requires reactive power compensation by means of shunt reactors in order to keep the voltage within the permissible limits. In most situations, particularly for long cable lengths, shunt reactors should be connected directly to the cable and energized together with the cable to minimize switching overvoltages and to control the capacitive current in the line breaker [1], [2].

The simultaneous energization of the cable and reactors may cause the zero-missing phenomenon, which means that the current through the line breaker does not cross zero value for several cycles (can last for several seconds). In this situation, it is difficult or even impossible to safely open the healthy phases if a fault occurs in the circuit at the instant of, or after, energization when the zero-missing current is still present. Therefore, the system is more vulnerable and unprotected against faults if proper countermeasures are not devised at the design stage of the cable project.

Several countermeasures are available for the zero-missing phenomenon, while each of those has advantages and disadvantages depending on the grid topology and specifications. Synchronized switching at voltage peak, sequential switching, and the use of circuit-breakers equipped with pre-insertion resistors are the mostly studied countermeasures in the literature [3]–[6].

In [3], switching at voltage peak is applied to avoid the zero-missing phenomenon based on an insulation coordination study. In [4], authors studied the use of pre-insertion resistors to minimize the zero-missing current, where they proposed a simple formula to approximate the resistor value. The expanded version of [4] is presented in [5], where some extra countermeasures of the zero-missing phenomenon are also discussed. An iterative process for more accurate calculation of the pre-insertion resistor size is provided in [5]. In [6], a general overview of the countermeasures and a more detailed study of the sequential switching countermeasure are provided.

There are three important aspects regarding countermeasures of the zero-missing phenomenon that have not been addressed in the literature: (a) the resulting transient overvoltages and inrush currents after applying a countermeasure, (b) the impact of the circuit-breaker mechanical delay on the effectiveness of an applied countermeasure, (c) the influence of hybrid OHL-Cable circuits and the cable length on the effectiveness of an applied countermeasure.

Furthermore, several countermeasures extra to the studied measures in the literature are available and have not been investigated so far. Under some circumstances, these methods can be the most effective solutions of the zero-missing phenomenon. Therefore, it is required to carry out a comprehensive study, which implements all countermeasures on a reference system and does a comparison based on a set of system operation criteria.

The goal of this paper is to address the mentioned scientific gaps by performing an in-depth investigation on countermeasures of the zero-missing phenomenon and determining the requirements, benefits, and deficiencies of each method. Countermeasures are compared in terms of resulting currents and

Manuscript received April 8, 2017; revised June 22, 2017; accepted July 16, 2017. Date of publication July 24, 2017; date of current version May 9, 2018. This work was supported by TenneT TSO B.V., Arnhem, The Netherlands, within the framework of the 380 kV cable research program. Paper no. TPWRD-00517-2017. *(Corresponding author: Hossein Khalilnezhad.)*

H. Khalilnezhad, M. Popov, and L. van der Sluis are with the Delft University of Technology, Delft 2628 CD, The Netherlands (e-mail: H.Khalilnezhad@tudelft.nl; M.Popov@tudelft.nl; L.vandersluis@tudelft.nl).

J. A. Bos and J. P. W. de Jong are with the TenneT TSO B.V., Arnhem 6800 AS, The Netherlands (e-mail: Jorrit.Bos@tennet.eu; Jan.P.de.Jong@tennet.eu).

A. Ametani is with Doshisha University, Kyoto 610-0321, Japan (e-mail: aametani@mail.doshisha.ac.jp).

Color versions of one or more of the figures in this paper are available online at http://ieeexplore.ieee.org.

Digital Object Identifier 10.1109/TPWRD.2017.2729883

voltages after their implementation. High transient overvoltages, a voltage dip/swell, and high inrush currents may occur when a particular countermeasure is applied. Applying a countermeasure should result in neither switching overvoltages nor inrush currents over the permissible limits.

Countermeasures are applied on a possible future hybrid OHL-Cable circuit in the Dutch 380 kV transmission system, for which the effect of the cable length on simulation results is studied. It is of high importance to take the impact of the cable length into account since a countermeasure may be the optimal solution only for a certain range of the cable length, depending on system specifications. Moreover, the switching sequence of breakers is determined for each countermeasure. This can be implemented in practice by applying controlled switching (also known as synchronized switching) and the use of single-pole operated circuit-breakers.

The paper is structured as follows: Section II elaborates basics of the zero-missing phenomenon and parameters affecting it; Section III discusses the developed model of the Dutch 380 kV grid for this study; Cable scenarios and operation criteria are presented in Sections IV and V, respectively. Section VI treats the simulation results, where countermeasures are analyzed and compared. The paper methodology and findings are discussed in Section VII, and finally, conclusions are presented in Section VIII.

II. Zero-Missing Phenomenon

The zero-missing phenomenon can be simply illustrated by the cable system (i.e., the cable and the shunt reactor) shown in Fig. 1. The cable system is energized by a voltage source.

When the reactor is energized, the charging current has two components, an ac-component and a decaying dc-component:

$$I_{SR}(t) = \underbrace{e^{-(\frac{R}{L})t}\left[\frac{-V_{\max}}{|Z|}\sin(\varphi-\theta)\right]}_{DC\ component} + \underbrace{\frac{V_{\max}}{|Z|}\sin(\omega t+\varphi-\theta)}_{AC\ component} \quad (1)$$

Where *R*, *L,* and *Z* are respectively resistance, inductance, and impedance of the reactor. $V_{\max}$ is the voltage amplitude, φ is the initial phase angle of the voltage (i.e., the point on the voltage waveform at which the breaker is closed), and θ is the load angle. As it is seen, the initial value of the dc-component depends on the initial phase angle and its decaying time depends on the time constant, expressed by $\tau = \frac{L}{R}$. The dc-component is maximum when $\varphi - \theta$ is 90° (at $t = 0$, equal to the amplitude of the ac-component), and is zero when $\varphi - \theta$ is zero.

The current through the circuit-breaker after the circuit is energized is as below:

$$I_{CB1}(t) = I_{SR}(t) + I_{cable}(t) = \underbrace{I_{SR,dc}(t)}_{DC\ comp.} + \underbrace{(I_{SR,ac}(t) + I_{cable}(t))}_{AC\ component} \quad (2)$$

$$I_{SR,ac}(t) = -K_{Sh} \times I_{cable}(t) \quad (3)$$

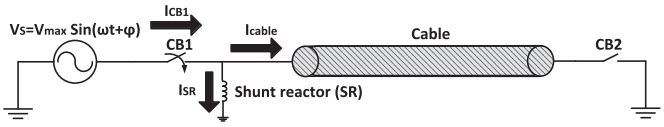

Fig. 1. Single-line diagram of a simple shunt compensated cable system.

Where I_{CB1} is the current through the circuit-breaker, I_{SR} is the energization current of the shunt reactor, I_{Cable} is the cable charging current. K_{Sh} is the shunt compensation degree and shows the percentage of the cable reactive power which is compensated by the shunt reactor. In (2) and (3), for simplicity, it is assumed the cable is a pure capacitor and the resistance of the shunt reactor is zero for the ac-component (these simplifications have a negligible influence).

As it is shown in (3), the ac-component of the reactor current has an opposite phase angle with the cable charging current. Therefore, in (2), the ac-component of the reactor current is partially (or completely if the compensation degree is 100%) cancelling out the cable charging current. When the compensation degree is higher than 50%, the ac-component in (2) may become smaller than the dc-component, so that the current does not cross the zero point until the dc-component is sufficiently damped. Thus, the zero-missing phenomenon can occur if two conditions are satisfied: (1) energization of the shunt reactor together with the cable, (2) shunt compensation degree larger than 50% ($K_{sh} > 50\%$).

Assume that the length of the cable in Fig. 1 is 60 km and the shunt compensation degree is 92.1% (obtained by a steady-state analysis for the sample cable [7]). The system is energized in two cases: closing each phase at zero voltage and closing each phase at voltage peak. This requires controlled switching and single-pole operated circuit-breakers. Resulting currents and voltages after energization at zero voltage and at voltage peak (obtained by PSCAD simulations) are respectively shown in Figs. 2 and 3.

Fig. 2(a) and (b) respectively show the cable charging current (I_{Cable}) and the shunt reactor current (I_{SR}), when each phase is closed at zero voltage. The dc-component of the shunt reactor current is maximum since $\varphi = 0$ and $\theta \cong 90°$ (see (1)). However, the reactor current always touches the zero point because the maximum dc-offset is equal to the amplitude of the ac-component. Fig. 2(c) shows the current through the circuit-breaker ($I_{CB1} = I_{Cable} + I_{SR}$). The total ac-component is very small due to the cancelation of 92.1% of the cable charging current by the ac-component of the reactor current. Thus, the total current flowing through the circuit-breaker is mainly dc and is not crossing the zero point. The main benefit of switching at voltage zero is that the cable charging inrush currents (Fig. 2(a)) and the transient switching overvoltages (Fig. 2(d)) are minimized.

In contrast, as shown in Fig. 3(b), the dc-component is zero if each phase is closed at voltage peak ($\varphi = 90°$ and $\theta \cong 90°$ in (1)). This means the zero-missing phenomenon does not occur (Fig. 3(c)). However, in comparison to the switching at zero voltage, the cable charging inrush currents (Fig. 3(a)) and the transient switching overvoltages (Fig. 3(d)) are higher.

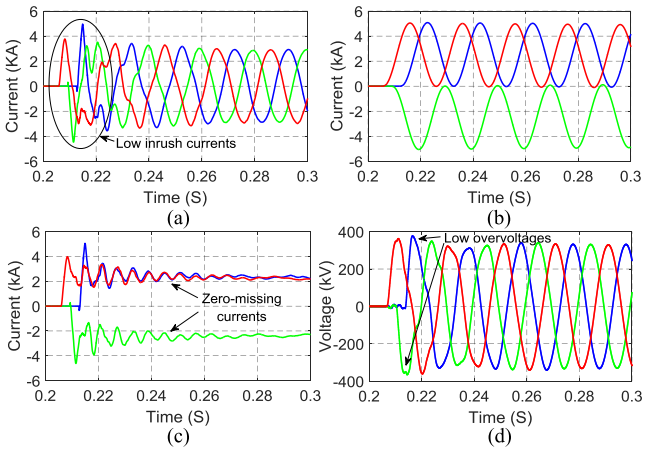

Fig. 2. Currents and open-end voltages after energization of the circuit in Fig. 1 (60 km cable, $K_{sh} = 92.1\%$). Each phase is closed at zero voltage. (a) Cable current, (b) Shunt reactor current, (c) Circuit-breaker current, and (d) Voltage at open-end.

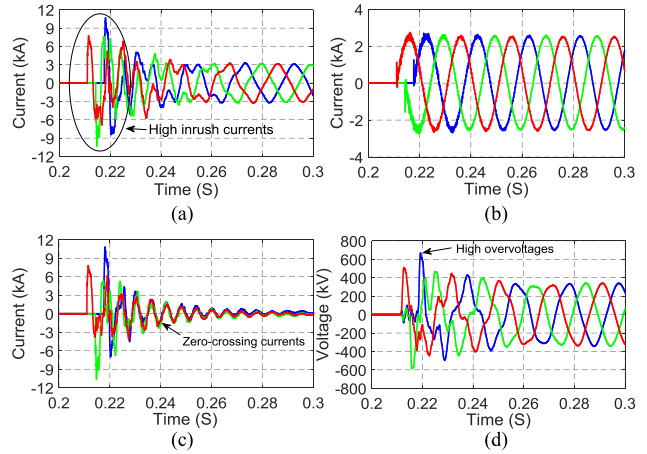

Fig. 3. Currents and open-end voltages after energization of the circuit in Fig. 1 (60 km cable, $K_{sh} = 92.1\%$). Each phase is closed at voltage peak. (a) Cable current, (b) Shunt reactor current, (c) Circuit-breaker current, and (d) Voltage at open-end.

III. Grid Modeling

A thorough frequency-dependent parameter model of the whole Dutch 380 kV transmission system is developed in PSCAD/EMTDC for the study of system transients in the time-domain. The frequency-dependent phase-domain model is applied to model OHLs and XLPE cables by the use of actual geometry data and electrical parameters. The grid model includes detailed representation of transformers and shunt reactors (shunt reactors are air core).

In the Dutch 380 kV grid, capacitor banks exist at some substations for voltage control and they are switched-in or out depending on the load-flow and voltage level. The 380 kV capacitor banks are represented by equivalent RLC circuits in the developed model of the grid.

Fig. 4 shows the structure of the hybrid OHL-Cable circuit under study. Cable sections are composed of two parallel cables per phase to achieve the same transmission capacity as the OHL

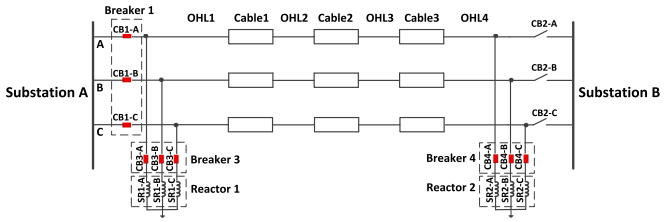

Fig. 4. Structure of shunt compensated hybrid OHL-Cable circuit.

TABLE I
Cable Scenarios and Shunt Reactor Sizes

Scenario	OHL length (km)	Cable length (km)	Compensation size (Mvar)		
			SR1	SR2	K_{Sh}
15% Cable	68	12	88	88	69.8%
25% Cable	60	20	178	178	84.8%
50% Cable	40	40	375	375	89.3%
75% Cable	20	60	580	580	92.1%
100% Cable	0	80	800	800	95.2%

sections. In addition, all cable cross-bondings are represented in full detail.

The three-phase shunt reactors are connected to the circuit right behind the line breakers and through breakers 3 and 4.

Having reactors connected to the circuit and behind the line breakers helps to limit energization overvoltages along the circuit and at the open-end as well as minimizing the capacitive (leading) current through the line breaker. In contrary, these are not achieved when the reactors are connected to the busbars or to the tertiary windings of power transformers at substations.

Separate breakers for shunt reactors results in an added switching flexibility as well as minimizing the risk of line resonance by decoupling reactors from the disconnected phase(s) or circuit. Resonance may occur between the reactor inductance, inter-phase/inter-circuit capacitance and cable capacitance if reactors remain connected to the disconnected phase(s) in uneven open-phase conditions (e.g., one phase is disconnected and the other two are energized) or to a fully three-phase disconnected circuit [8]. The risk of ferroresonance exists too in case of magnetic core reactors. Thus, these risks can be minimized by disconnecting the shunt reactors from the disconnected phase(s)/circuit when reactors are connected via breakers.

IV. Cable Scenarios and Shunt Compensation

Five cable scenarios for the hybrid OHL-Cable circuit are considered to determine the cable length influence on the effectiveness of countermeasures. In these scenarios, the cable share varies from 15% to 100% (fully cable) of the transmission length. The total transmission length of the hybrid circuit from the substation A to substation B is 80 km.

The cable scenarios and the compensation sizes are presented in Table I. SR1 and SR2 are referring to the three-phase shunt reactors at the substations A and B, respectively, and the reported values for each of them is the total three-phase size. The required

shunt compensation for each cable scenario is determined by a detailed steady-state analysis presented in [7].

V. Operation Criteria

The implementation of a countermeasure can cause high inrush currents and/or high transient switching overvoltages. High inrush currents or very steep and high voltage surges increase dielectric and mechanical stresses on circuit-breakers and other system components [9]. These stresses can cause immediate or gradual damages on equipment and affect system reliability.

It is important to define clear criteria based on the system operation limits and standards to evaluate voltages and currents after implementation of a countermeasure. Therefore, three criteria are defined based on the requirements specified by manufacturers, the IEC standards, and the grid code for circuit-breakers, insulation coordination, and power quality:

1) *Amplitude and frequency of inrush current*: the countermeasure should not cause high inrush currents recognized to be harmful for breakers and other components [9], [10]. For capacitor banks, standardized peak value and frequency of capacitive inrush currents are 20 kA and 4.25 kHz, respectively [10], [11]. These values are used in this paper since cable energization inrush current is almost similar to that of an equivalent capacitor bank. However, it should be noted that the amplitude and the rate-of-rise of cable inrush current are normally lower than those of an equivalent capacitor bank due to the relatively higher surge impedance of cables [9].
2) *Transient switching overvoltages*: the peak values of the phase-to-earth transient energization overvoltages after implementation of a countermeasure should remain below the switching impulse withstand voltage (SIWV) of 3.38 pu (1050 kV) [12].
3) *RMS voltage step*: the IEC standard [13] and the Dutch grid code are imposing limits for the quick changes in RMS voltage between two steady-states. This criterion is mainly related to power quality and minimization of the disturbance to consumers. After switching, RMS voltages should be within the voltage dip and swell thresholds of 0.9 pu (342 kV) and 1.1 pu (418 kV), respectively. The *Rapid Voltage Change (RVC)* should be smaller than 3% (11.4 kV). The time frame for calculation of the RMS value is half of the power-frequency cycle (10 ms in 50 Hz systems).

VI. Countermeasures and Simulation Results

The main goal of this paper is to analyze and compare different countermeasures of the zero-missing phenomenon. The countermeasures fall into one of the following three categories:

1) *Prevention methods*: the zero-missing current will be avoided by application of these countermeasures.
2) *Mitigation methods*: these measures do not prevent the occurrence of the zero-missing current, but they minimize the decaying time of the dc-component by increasing the system damping (i.e., smaller time constant), so that the current through the breaker crosses the zero point faster.
3) *Handling methods:* these measures are neither helping to avoid nor to mitigate the zero-missing current. However, they help system operators to safely open the breakers when a fault occurs in the hybrid circuit at the instant of, or after, energization when the zero-missing phenomenon is still present.

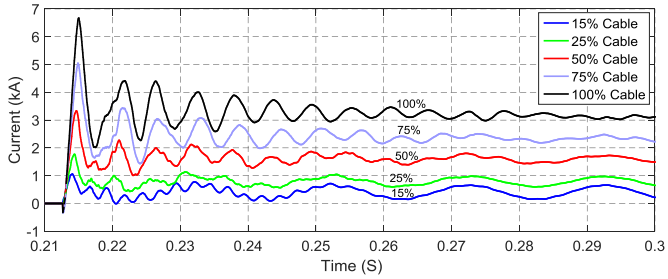

Fig. 5. Line breaker current (I_{CB1}, phase A) for different cable scenarios when each phase is energized at zero voltage.

Six countermeasures are studied in this paper: (1) simultaneous cable and reactor energization at voltage peaks, (2) in advance cable energization, (3) in advance reactor energization, (4) sequential switching, (5) opening of the faulted phase(s), and (6) increasing the dc-offset damping. Each measure is first elaborated and then simulation results are presented.

Transient overvoltages are expressed in per unit, where the base value (1 pu) is the peak value of the phase-to-earth nominal voltage (i.e. 1 pu $=$ 310.27 kV). Overvoltages are recorded at the open-end (unless differently specified) since the highest overvoltages are occurring there.

Fig. 5 shows the current through the line breaker for different cable scenarios when each phase is energized by controlled switching at zero voltage. With increasing cable share, the zero-missing phenomenon becomes more severe in terms of the amplitude of the dc-component and the required time for the first zero crossing. This is due to the larger dc-component (because of bigger compensation size in Mvar, i.e., smaller $|Z|$ in (1)) and a very small ac-component (because of high degree of compensation) for longer cables. As the result, the current through the line breaker is dominantly a high-amplitude and low-damped dc current.

A. Simultaneous Cable and Reactor Energization at Voltage Peaks

This technique proposes to energize each cable phase together with shunt reactors of that phase at its voltage peak (needs controlled switching and single-pole operated breakers). This is a prevention countermeasure, but higher switching overvoltages and higher inrush currents are expected due to energization at voltage peaks. Fig. 6 shows the resulting current when this measure is applied. With increasing cable length, the inrush current peak value gets higher (around 13 kA for 100% cable (80 km)) due to the larger circuit capacitance; however, the inrush current peak values and the frequencies are within the specified limits.

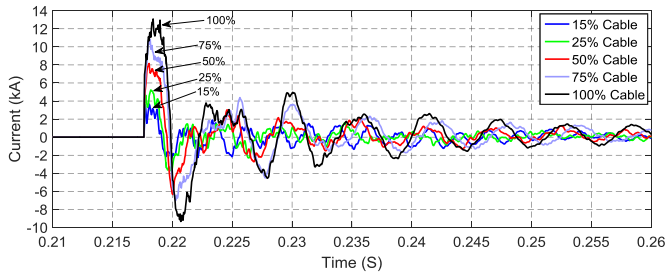

Fig. 6. Line breaker current (I_{CB1}, phase A) for different cable scenarios when each phase is energized at voltage peak (Countermeasure A).

TABLE II
OVERVOLTAGES AFTER CLOSING EACH PHASE AT VOLTAGE PEAK

Scenario	Maximum overvoltage (pu)					
	Synchronized switching at zero voltage			Synchronized switching at voltage peak		
	Phase A	Phase B	Phase C	Phase A	Phase B	Phase C
15% Cable	1.128	1.186	1.199	2.159	1.650	2.182
25% Cable	1.125	1.202	1.141	1.973	2.056	1.724
50% Cable	1.128	1.193	1.147	2.224	2.111	1.682
75% Cable	1.215	1.180	1.170	2.153	1.892	1.647
100% Cable	1.209	1.135	1.151	2.063	1.763	1.615

Table II shows the maximum overvoltages at the open-end. In some cases, the resulting overvoltages by switching at voltage peak are almost double of those resulted by switching at zero voltage. Although the overvoltages are higher, they are still below the specified limit of 3.38 pu.

It should be pointed out that the resulting overvoltages are dependent on the system topology and parameters such as number/location/length of OHL and cable sections, power-frequency voltage, and short-circuit power. The distribution and length of OHL and cable sections can significantly affect the resulting overvoltages due to the changes in reflections and refractions of the propagating wave at the transition points.

This technique requires an accurate controlled switching to close each pole of the breaker at its voltage peak. In practice, breakers are not ideal and they show variations in their operating times [9], [11]. Variations in the operating time are either predictable or stochastic. Predictable variations (e.g., long-term aging) do not affect the effectiveness of controlled switching and can be compensated by an adaptive control. However, stochastic variations (inherent scatter) of the operating time can result in energization of the cable and reactors at a point different than the voltage peak. This limitation of controlled switching can be described by the statistical distribution function of the scatter [9].

A statistical analysis is carried out to find the influence of stochastic variations in the breaker closing time on the probability distribution of energization overvoltages. For each breaker pole, the closing time is varied by a normal (Gaussian) distribution. The mean value is the instant at which the voltage peak of that pole occurs, the standard deviation (σ) is 1 ms, and the distribution curve is truncated at -3σ and $+3\sigma$. 50 closing times are simulated for each pole to obtain an accurate set of statistical data [3], [9], [14]. Statistical simulations are implemented in PSCAD by the use of multiple-run feature and random number generators based on the normal distribution.

TABLE III
KEY VALUES OF THE ENERGIZATION OVERVOLTAGE DISTRIBUTIONS

Scenario	Overvoltage (pu)			
	Max.	Mean	Standard deviation (σ)	2% value
15% Cable	2.406	1.879	0.279	2.393
25% Cable	2.378	1.755	0.271	2.283
50% Cable	2.355	1.861	0.216	2.134
75% Cable	2.188	1.850	0.248	2.181
100% Cable	2.151	1.818	0.218	2.132

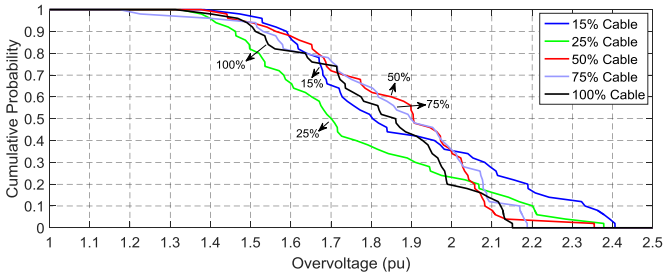

Fig. 7. Cumulative probability distributions of overvoltages due to stochastic variations in the breaker closing time.

Table III shows the maximum, mean, standard deviation, and 2% values of the obtained overvoltage distributions for different cable scenarios. The 2% value is the overvoltage value that the probability of this value being exceeded is 2% [15]. From each energization simulation, the peak value of the overvoltage on each phase-to-earth is included in the overvoltage probability distribution (known as the phase-peak method [15]). The maximum recorded overvoltage is 2.406 pu, which is below the specified limit.

Fig. 7 shows the cumulative probability of overvoltages obtained by the statistical variation of the closing time. For a given voltage level, the vertical axis shows the cumulative probability of overvoltages exceeding that voltage level.

When the stochastic variation in the pole closing time exceeds a threshold, the cable and reactors are energized at a point on the voltage waveform at which the dc-component of the line breaker current is larger than the ac-component. This means that the zero-missing current occurs, although it was supposed to be avoided by energizing at voltage peak as the aiming closing point. Therefore, this countermeasure will be successful only if the stochastic variation in the breaker closing time is not exceeding a threshold. This threshold is named here *breaker closing variation threshold (BCVT)*.

The BCVT shows the maximum variation in the breaker closing time around the instant of voltage peak so that the breaker current crosses the zero point before a given time limit. If the pole is not closed at $T_{peak} - \Delta T_{BCVT} < T <$

TABLE IV
BCVT FOR DIFFERENT TIME LIMITS

Scenario	Time limit								
	10 ms	20 ms	40 ms	60 ms	80 ms	100 ms	500 ms	1 s	2 s
15% Cable	±0.71 ms (±12.8°)	±1.42 ms (±25.6°)	±1.43 ms (±25.7°)	±1.43 ms (±25.8°)	±1.44 ms (±25.9°)	±1.45 ms (±26°)	±1.54 ms (±27.7°)	±1.67 ms (±30°)	±1.67 ms (±30°)
25% Cable	±0.21 ms (±3.7°)	±0.57 ms (±10.3°)	±0.57 ms (±10.3°)	±0.58 ms (±10.4°)	±0.58 ms (±10.4°)	±0.58 ms (±10.5°)	±0.64 ms (±11.6°)	±0.72 ms (±13°)	±0.87 ms (±15.7°)
50% Cable	±0.13 ms (±2.3°)	±0.38 ms (±6.8°)	±0.38 ms (±6.9°)	±0.38 ms (±6.9°)	±0.39 ms (±7°)	±0.39 ms (±7.1°)	±0.46 ms (±8.3°)	±0.55 ms (±9.9°)	±0.69 ms (±12.5°)
75% Cable	±0.08 ms (±1.5°)	±0.27 ms (±4.8°)	±0.27 ms (±4.9°)	±0.27 ms (±4.9°)	±0.28 ms (±5°)	±0.28 ms (±5.1°)	±0.35 ms (±6.3°)	±0.43 ms (±7.7°)	±0.53 ms (±9.6°)
100% Cable	±0.04 ms (±0.8°)	±0.15 ms (±2.7°)	±0.16 ms (±2.8°)	±0.16 ms (±2.8°)	±0.16 ms (±2.9°)	±0.16 ms (±2.9°)	±0.21 ms (±3.8°)	±0.27 ms (±4.8°)	±0.32 ms (±5.8°)

$T_{peak} + \Delta T_{BCVT}$, the absolute value of the dc-component of the current through the line breaker will be larger than the absolute value of the ac-component, so that the total current does not cross the zero point before the given time limit. The time limit can be defined based on the preference of the system operator.

For calculation of the BCVT, first the line breaker current should be calculated as a function of the breaker closing time. This can be done by the use of system parameters including the OHL and cable impedances, shunt reactor impedance, and shunt compensation degree. Then, the maximum variation in the breaker closing time around the instant of voltage peak, for which the line beaker current has a first zero-crossing before the given time limit, is calculated by an iterative process. This means that the BCVT is calculated under the condition that the zero-missing current must not occur after closing, or if it occurs, it should disappear within the given time limit after the closing time.

Table IV shows the calculated BCVT for different time limits and the five cable scenarios. The values in parentheses are the corresponding angles in degrees. As it is shown, for a given cable length, BCVT increases when the time limit increases.

For a given time limit, the BCVT is smaller for longer cables since the higher degree of compensation required for longer cables results in a line breaker current with a small ac-component but a large dc-component (see Fig. 5). The dominant dc-component is very low-damped (due to the large time constant of shunt reactors) and sensitive to variations of the closing time. In other words, in (1), any change in $\sin(\varphi - \theta)$ is magnified by $\frac{V_{\max}}{|Z|}$, which is larger for longer cables due to bigger compensation size (i.e., smaller |Z|). Thus, for longer cables, any variation in the closing time has a more noticeable impact on the dc-component of the line breaker current.

Knowing the BCVT is crucial because it specifies the accuracy of breakers used for the countermeasure. In some cases, a countermeasure is not a reliable solution if the breaker delay can exceed the BCVT.

B. Energization in Sequence

The zero-missing phenomenon can be avoided when the shunt reactors are energized with an intentional delay before or after the cable energization instant. The main drawbacks of the previous countermeasure, in which both cable and reactors were energized together at voltage peaks, were high transient overvoltages and inrush currents. However, with a controlled time delay between energizations, not only transient overvoltages can be minimized by energizing the cable at zero voltage, also the zero-missing current can be avoided by energizing the reactors at voltage peak.

The key parameter for the success of this countermeasure is to keep the time delay between energization of the cable and energization of the shunt reactors as short as possible. Otherwise, a voltage dip/swell, a RVC larger than 3%, and under/over excitation of nearby generators are expected [2].

This prevention countermeasure can be realized in two ways, depending on whether cable or reactor is energized first. They are named *in advance cable energization* and *in advance reactor energization* countermeasures. The application of these methods requires controlled switching and single-pole operated breakers. Breakers planned to close at voltage peaks (i.e., reactor breakers) should be tested to comply with the BCVT to ensure that the zero-missing current is avoided. However, breakers switching at zero voltage should not necessarily comply with the BCVT requirement since they do not affect the dc-offset of the current.

B.1 In Advance Cable Energization

In this countermeasure, each cable phase is energized at zero voltage and a quarter of a cycle later (5 ms in a 50 Hz system), at the voltage peak, the reactors of that phase are energized. Voltage at the open-end and the line breaker current after applying this countermeasure are shown for the 75% cable scenario (60 km cable) in Fig. 8. The results are compared with those of the Countermeasure A (i.e., simultaneous cable and reactor energization at voltage peaks). The transient overvoltage and the inrush current are considerably lower with this countermeasure since the cable is energized at zero voltage. The main advantage of this measure is minimization of the stress on the breaker and system components.

The results in Fig. 8 are for the case at which the time delay between cable energization and reactors energization is 5 ms (optimal case); however, the delay may be longer in practice.

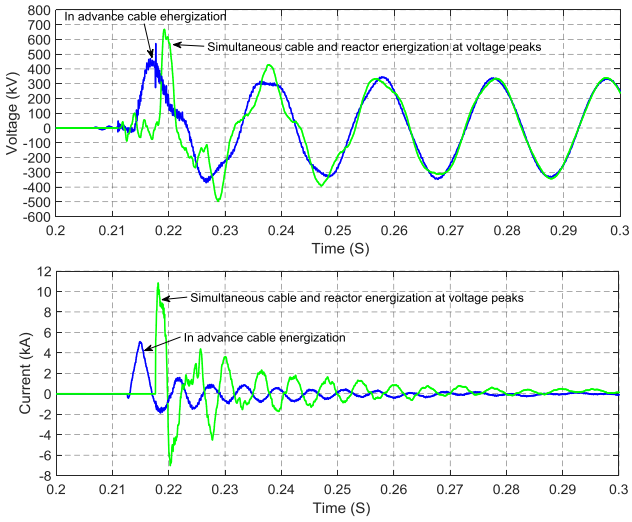

Fig. 8. Open-end voltage (phase A) and line breaker current (I_{CB1}, phase A) after implementation of the Countermeasure B.1 (with 5 ms delay) and the Countermeasure A (75% cable scenario, $K_{sh} = 92.1\%$).

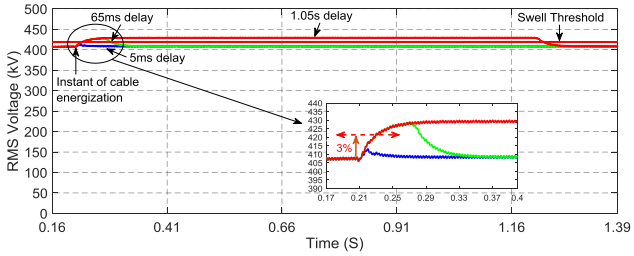

Fig. 9. RMS voltage step at the substation A after implementation of the Countermeasure B.1 with three different time delays (75% cable scenario, $K_{sh} = 92.1\%$).

RVC and voltage swell can exceed the limits when the time delay becomes sufficiently long.

Fig. 9 shows the RMS voltage step at the substation A after energizing the 75% cable scenario (60 km cable) with three time delays: 5 ms, 65 ms (3+1/4 of a cycle), and 1.05 s (5+1/4 of a cycle). With both 65 ms and 1.05 s delays, the voltage step exceeds the 3% limit and goes beyond the swell threshold of 1.1 pu $(1.1 \times 380\ \text{kV} = 418\ \text{kV})$. Such a high sensitivity to delay is the result of the high steady-state voltage of 1.076 pu before closing, leaving a margin of 0.024 pu for the voltage step.

In addition to the initial voltage before closing, the cable length and the short circuit strength of the substation from which the cable system is energized are affecting the amplitude of the voltage step. The effect of cable length on voltage step, when the time delay is 1.05 s, is shown in Fig. 10. Only voltage steps of 15% and 25% cable scenarios are below the 3% and 1.1 pu limits, whereas with increasing cable length the step exceeds both limits. Therefore, the main limitation of this countermeasure is large voltage steps in the case of long delays.

B.2 In Advance Reactor Energization

The implementation of this countermeasure requires two additional single-pole operated breakers to be installed on both

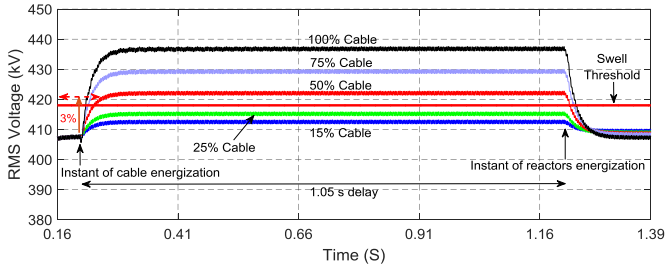

Fig. 10. RMS voltage step at the substation A after energizing different cable scenarios with the Countermeasure B.1. The time delay is 1.05 s.

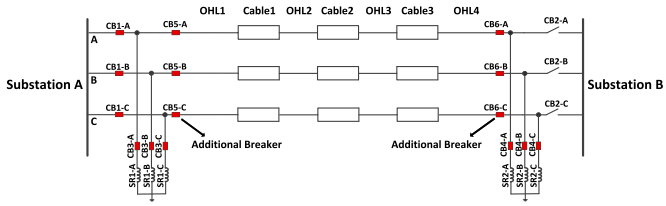

Fig. 11. Structure of shunt compensated hybrid OHL-Cable circuit for the Countermeasure B.2.

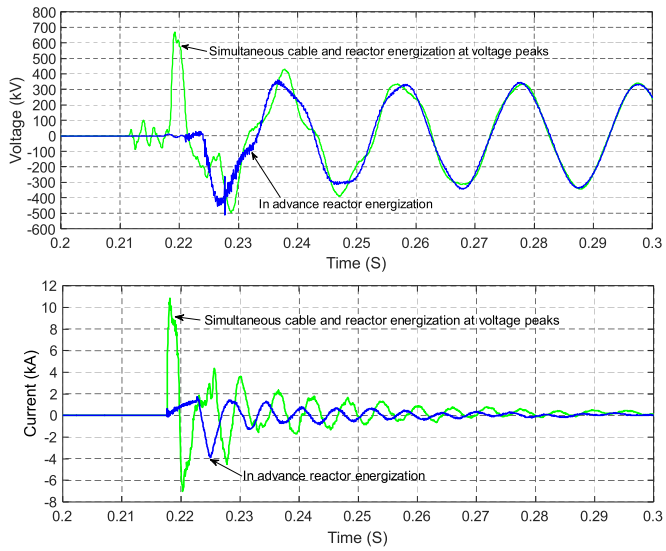

Fig. 12. Open-end voltage (phase A) and line breaker current (I_{CB1}, phase A) after implementation of the Countermeasure B.2 (with 5 ms delay) and the Countermeasure A (75% cable scenario, $K_{sh} = 92.1\%$).

sides of the hybrid circuit, as shown in Fig. 11. This allows that breakers 1 and 3 be closed at voltage peak to energize the reactor 1 (SR1) before the cable is energized. After 5 ms delay, the additional breaker, which is installed at the beginning of OHL1, will be closed at zero voltage to energize the cable. At the next voltage peak after cable energization, the second shunt reactor (i.e., reactor 2) is energized by closing breaker 4 and the other additional breaker, which is installed at the end of OHL4. Since both reactors are energized at voltage peak, the zero-missing phenomenon is prevented.

Fig. 12 shows the open-end voltage and the line breaker current after energization of the 75% cable scenario (60 km cable) when this countermeasure is applied. The transient overvoltage

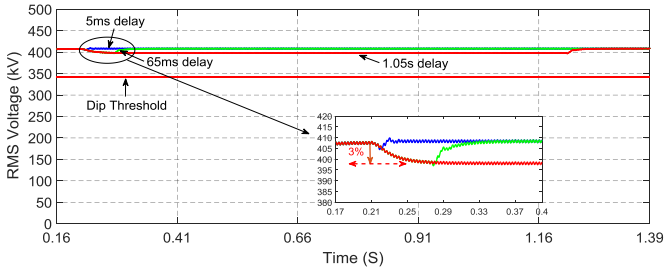

Fig. 13. RMS voltage step at the substation A after implementation of the Countermeasure B.2 with three different time delays (75% cable scenario, $K_{sh} = 92.1\%$).

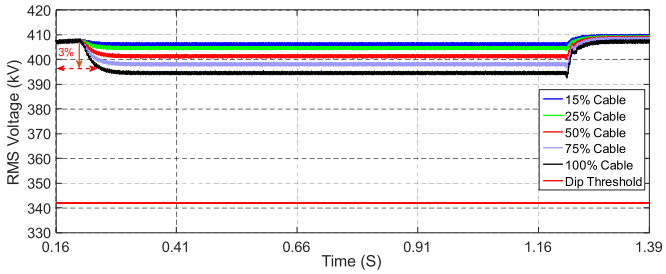

Fig. 14. RMS voltage step at the substation A after energizing different cable scenarios with the Countermeasure B.2. The time delay is 1.05 s.

and the inrush current are considerably lower compared to those of the previous countermeasures.

Fig. 13 shows the voltage step at the substation A after energization of the 75% cable scenario with time delays of 5 ms, 65 ms, and 1.05 s. Unlike the Countermeasure B.1 (i.e., in advance cable energization), the voltage step is not exceeding the 3% limit and is also far above the dip threshold (0.9 pu). The reason for not exceeding the 3% limit is the size of reactor 1 (SR1), which according to Table I is between 34.9% to 47.6% of cable reactive power. Thus, in advance energization of SR1 has a very smaller influence on voltage than the case of cable energization in advance. The reason for not exceeding the dip threshold, in addition to comparatively small size of SR1, is the high power-frequency voltage before energization (1.076 pu). As Fig. 14 shows, the 3% limit is only exceeded when the cable share is 100% (80 km).

It can be concluded that this countermeasure has less negative consequences than the previous measures in regard to the specified operation criteria.

C. Sequential Switching

Sequential switching is a handling countermeasure, which applies remedial switching operations to protect the system in the case a fault occurs in the circuit during the zero-missing phenomenon [6]. By applying this measure, the cable and reactors are energized together at zero voltage (by the use of controlled switching and single-pole operated breakers) to minimize the transient overvoltages and the inrush currents.

When a fault occurs in the circuit during energization, the line breaker(s) of the faulted phase(s) can interrupt the current since it crosses the zero point. In fact, the fault current is superimposed on the ac-component of the current through the line

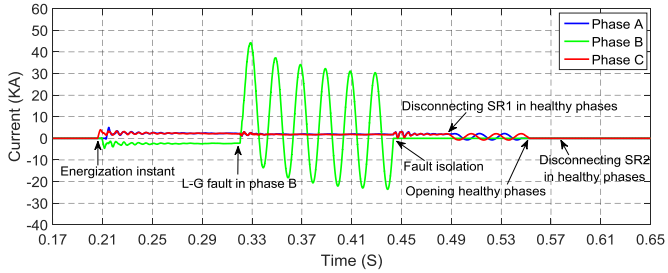

Fig. 15. Line breaker current (I_{CB1}) when the sequential switching countermeasure is applied (75% cable scenario, $K_{sh} = 92.1\%$).

breaker and therefore the total ac-component becomes larger than the dc-component. However, the line breaker(s) of healthy phase(s) cannot interrupt the current due to the zero-missing phenomenon.

In order to open the line breaker(s) of healthy phase(s), the degree of compensation should be decreased to 50% or less. When the compensation degree is dropped to 50% or less, the ac-component of the line breaker current becomes larger than the dc-component, so that the line current crosses the zero point. The decrease of compensation degree to 50% is the preferred case; in fact, the leading current through the line breaker and overvoltages along the circuit are more reduced compared to the case in which the degree of compensation is lower than 50%. Moreover, to limit the overvoltages, it is preferable not to disconnect the reactors at the open-end.

The line breakers should be type-tested for higher capacitive (leading) current interruption capability since after the decrease of the compensation degree to 50% or less, the capacitive current flowing through the line breaker can be large (e.g., for 60 km cable with 50% compensation, the capacitive current through the line breaker is about 1 kA). A drawback of this countermeasure is that the zero-missing problem is transferred to the next set of breakers when a line breaker of a healthy phase fails. Current differential relays are also required for realization of this countermeasure [6].

As an example of this countermeasure, assume that the hybrid circuit with 75% cable (60 km cable) and the reactors are energized together at zero voltage. A single-line-to-ground (SLG) fault is applied at t = 0.32 s in phase B of OHL 3 (see Fig. 4). Fig. 15 shows the current through the line breaker when the sequential switching countermeasure is applied. The breaker of phase B (CB1-B) is opened by the protection scheme 120 ms after fault occurrence. The application of this countermeasure does not cause high transient overvoltages and inrush currents since the cable and reactors are energized at voltage zero.

It is worth mentioning that the currents through the reactor breakers of the faulted phase(s) are not crossing the zero point since reactors are discharging into the fault. So, as a common practice [16], reactor breakers do not operate until the reactor currents cross the zero point.

D. Opening of the Faulted Phase(s)

In this handling countermeasure, only the line breaker(s) of the faulted phase(s) is/are opened when a fault occurs in the

circuit. The healthy phase(s) is/are opened after the dc-offset is sufficiently damped and the line breaker current crosses the zero point.

The main benefit of this countermeasure is that it is cheap and only needs single-pole operated breakers, which are already commonly used in transmission systems. However, the waiting time for damping of the dc-component in healthy phase(s) can be up to several seconds due to the large time constant of shunt reactors. Leaving healthy phase(s) connected to the system may cause resonance in the disconnected phase(s) after the fault is removed [8]. In addition, applying this measure on cable projects near a generator may not be possible as this measure causes a prolonged unbalanced operation [6].

E. Increasing the DC-Offset Damping

The total X/R ratio of the cable systems is large, resulting in a low damped dc-offset. In this mitigation countermeasure, the X/R ratio and as the result the dc-offset damping time are decreased by using an additional resistor. In addition, the cable and reactors are energized together at zero voltage to minimize the overvoltages and the inrush currents.

One way of adding the resistor is to use a breaker equipped with the pre-insertion resistor (closing resistor) for the line or shunt reactors [9], [11]. The resistor (which its size can be in the order of the line surge impedance [16]) is connected through an auxiliary contact in parallel with the main contact (breaking chamber), as shown in Fig. 16(a). The circuit is energized through the resistor for a few milliseconds (e.g., approximately 8–12 ms for ABB breakers [11]) before closure of the arcing contact. These breakers are more expensive than the ordinary breakers and controlled switching. The cost can be even much higher if a new breaker is needed to be developed.

As an alternative case, a separate resistor can be connected in series with an ordinary beaker. The resistor is bypassed by a parallel disconnector or breaker as shown in Fig. 16(b). The breaker can be a lower voltage breaker with 380 kV insulation since it is not supposed to interrupt a fault current. The main advantage of this topology is controllability of the resistor bypass time. However, an additional cost for the purchase of an extra breaker/disconnector and the resistor is imposed.

Fig. 17 shows the influence of the pre-insertion resistor size on the dc-component of the line breaker current when each phase of the circuit with 75% cable (60 km cable) is energized at zero voltage. The dc-component decreases faster with increasing resistor size; however, it is crucial to find the optimum size of the resistor to increase the effectiveness and to minimize the cost. Large resistors act as an open-circuit and small resistors do not cause any improvement in the dc-offset damping.

Reference [5] has proposed an iterative process to solve differential equations for calculation of the pre-insertion resistor value. A formula based on energy equations (energy that the pre-insertion resistor should dissipate) is also proposed in [4] and [5]. This formula gives an approximation of the resistor value without being required to perform the iterative process, although is not always accurate due to simplifications.

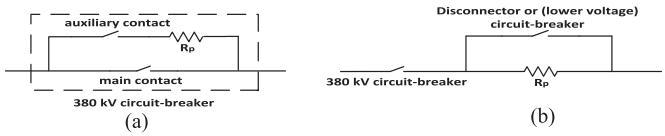

Fig. 16. Use of resistors to mitigate the zero-missing phenomenon, (a) a circuit-breaker equipped with the pre-insertion resistor, (b) a resistor in series with an ordinary circuit-breaker.

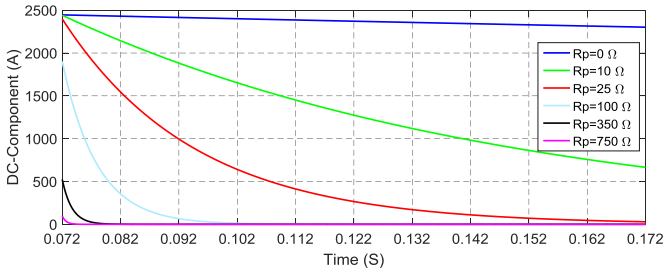

Fig. 17. Dc-component of the line breaker current ($\mathrm{I_{CB1}}$) for different pre-insertion resistor sizes when each phase is energized at zero voltage (75% cable scenario, $K_{sh} = 92.1\%$).

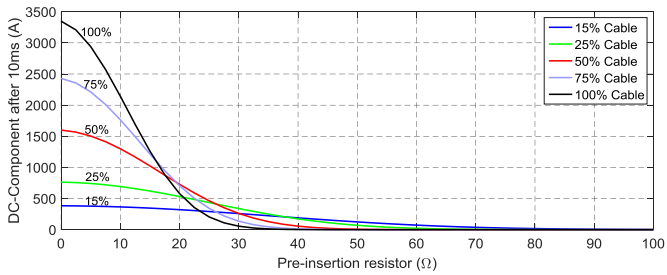

Fig. 18. Dc-component of the line breaker current ($\mathrm{I_{CB1}}$) after 10 ms versus the size of the pre-insertion resistor for different cable scenarios. Each phase is energized at zero voltage.

If a breaker equipped with the pre-insertion resistor (Fig. 16(a)) is used, the resistor should be sized so that the zero-missing phenomenon disappears by the resistor bypass instant. Fig. 18 shows the dc-component after 10 ms (average of 8–12 ms [5], [11]) versus the size of pre-insertion resistor for different cable scenarios when each phase is closed at zero voltage. The drop of the dc-component is steeper for longer cables when the resistor size is increased. This is due to the smaller X/R ratio of systems with longer cables, in which adding an additional resistance has a more remarkable impact.

The main limitation of this countermeasure is the thermal design of the resistor. The dissipated power in the resistor is shown in Fig. 19. This countermeasure requires special designed resistors to tolerate a huge power dissipation for a couple of milliseconds. This imposes extra costs and complexity to the countermeasure.

VII. Discussion

Several countermeasures of the zero-missing phenomenon were analyzed and compared. The applied methodology and

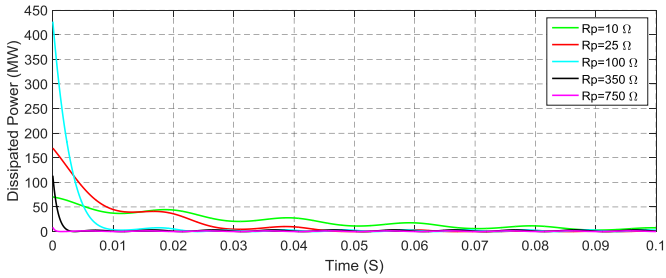

Fig. 19. Dissipated power in different pre-insertion resistor sizes when each phase is energized at zero voltage (75% cable scenario, $K_{sh} = 92.1\%$).

findings are applicable on any network since the study is based on practical assumptions like the use of a hybrid OHL-Cable circuit and the three system operation criteria. Moreover, simulation results are obtained by electromagnetic transient (EMT) studies on a model of an actual power transmission grid. It should be stressed that the influence of system topology and parameters (like the configuration of hybrid OHL-Cable circuit, power-frequency voltage, short-circuit power, etc.) on the effectivity of a countermeasure should always be considered.

Some of the countermeasures need special designed circuit-breakers, control strategies and resistances, which can impose extra costs and complexity on the system design and operation. The implementation of the Countermeasures B.1 and B.2 is more sophisticated than commonly applied techniques like the Countermeasure A since they require multiple control systems, which are coordinated together with a communication system. The advantages of these countermeasures over a traditionally used method, in terms of resulting overvoltages and inrush currents, are validated in Figs. 8 and 12, where the results are compared with those of the Countermeasure A.

VIII. Conclusion

This paper studied the effectiveness of six countermeasures of the zero-missing phenomenon in (E)HV cable systems. It was shown that the zero-missing phenomenon becomes more severe by increasing the cable share in the hybrid OHL-Cable circuit.

Simultaneous energization of the cable and reactors at voltage peaks is a common prevention countermeasure; however, the resulting transient overvoltages and inrush currents should be investigated. To decrease the transient overvoltages and inrush currents, *energization in sequence*, as a prevention countermeasure, can be applied. A voltage dip/swell is the main risk of applying this countermeasure for long cable lengths. As an example, for the studied cable system, this situation occurs for cables longer than 50 km when cable is energized first. The impact of stochastic variations in the breaker closing time on overvoltages should be assessed by a statistical analysis. Moreover, breakers operating at voltage peak should be tested for BCVT.

Other countermeasures are *sequential switching* (handling measure), *opening of the faulted phase(s)* (handling measure), and *increasing the dc-offset damping* (mitigation measure). These methods result in low transient overvoltages and inrush currents. The later one is a costly measure for which the thermal design of the resistor is a challenge.

For the investigated cable system, *in advance reactor energization* and *sequential switching* are concluded as the most effective and less risky countermeasures resulting in low transient overvoltages and low inrush currents.

Finally, the countermeasure effectiveness should always be investigated for each cable project by a similar study since the system specifications may change from one case to another affecting the consequent voltages and currents.

References

[1] CIGRE Working Group C4.502, "Power system technical performance issues related to the application of long HVAC cables," CIGRE Tech. Brochure No. 556, Oct. 2013.
[2] H. Khalilnezhad, M. Popov, J. A. Bos, and K. P. J. Jansen, "Influence of partial undergrounding on the transient stability of EHV power transmission systems," *Elect. Power Syst. Res.*, vol. 131, pp. 126–138, 2016.
[3] U. S. Gudmundsdottir and P. B. Holst, "Solving zero-missing with cable energization at voltage peak, based on insulation coordination study results," in *Proc. Int. Conf. Power Syst. Transients*, Vancouver, BC, Canada, Jul. 2013, pp. 1–6.
[4] F. F. da Silva, C. L. Bak, U. S. Gudmundsdottir, W. Wiechowski, and M. R. Knardrupgard, "Use of a pre-insertion resistor to minimize zero-missing phenomenon and switching overvoltages," in *Proc. IEEE Power Energy Soc. Gen. Meeting*, Calgary, AB, Canada, Oct. 2009, pp. 1–7.
[5] F. F. da Silva, C. L. Bak, U. S. Gudmundsdottir, W. Wiechowski, and M. R. Knardrupgard, "Methods to minimize zero-missing phenomenon," *IEEE Trans. Power Del.*, vol. 25, no. 4, pp. 2923–2930, Oct. 2010.
[6] A. Ametani, T. Ohno, and N. Nagaoka, *Cable System Transients: Theory, Modeling and Simulation*. Hoboken, NJ, USA: Wiley, Jul. 2015.
[7] H. Khalilnezhad, S. Chen, M. Popov, J. A. Bos, J. P. W. De Jong, and L. Van Der Sluis, "Shunt compensation design of EHV double-circuit mixed OHL-cable connections," in *Proc. IET Int. Conf. Resilience Transm. Distrib. Netw.*, Birmingham, U.K., 2015, pp. 1–6.
[8] CIGRE Working Group C4.307, "Resonance and feroresonance in power networks," Brochure no. 569, Feb. 2014.
[9] R. Smeets, L. van der Sluis, M. Kapetanovic, D. Peelo, and A. Janssen, *Switching in Electrical Transmission and Distribution Systems*. Hoboken, NJ, USA: Wiley, 2015.
[10] High-voltage Switchgear and Controlgear-Part 100: Alternating-Current Circuit-Breakers, IEC 62271–100, 2008.
[11] *Live Tank Circuit Breakers: Buyer's Guide*, 6th ed., ABB, Ludvica, Sweden, 2014.
[12] Insulation Co-Ordination-Part 1: Definitions, Principles and Rules, IEC 60071–1, 2006.
[13] Electromagnetic Compatibility (EMC)-Part 4-30: Testing and Measurement Techniques-Power Quality Measurement Methods, IEC 61000-4-30, 2006.
[14] T. Ohno, C. L. Bak, A. Ametani, W. Wiechowski, and T. K. Sorensen, "Statistical distribution of energization overvoltages of EHV cables," *IEEE Trans. Power Del.*, vol. 28, no. 3, pp. 1423–1432, Jul. 2013.
[15] Insulation Co-Ordination-Part 2: Application Guide, IEC 60071-2, 1996.
[16] *Live Tank Circuit Breakers: Application Guide*, 1.2 ed., ABB, Ludvica, Sweden, 2013.

Hossein Khalilnezhad (GSM'12) was born in Iran in 1987. He received the B.Sc. degree in electrical engineering from the Shiraz University of Technology, Shiraz, Iran, and the M.Sc. degree (*cum laude*) in electrical power engineering from the Delft University of Technology, Delft, The Netherlands, in September 2013. He is currently working toward the Ph.D. degree at the Delft University of Technology, where he studies EHV underground cable systems. Mr. Khalilnezhad won the Shell Master Award for the best M.Sc. thesis in the field of innovation and technology in March 2014. He was awarded the IEEE PES Travel Grant at the POWERCON 2017 Conference in Australia in September 2016.

Marjan Popov (M'95–SM'03) received the Dipl. Ing. degree from the University of Skopje, Skopje, Republic of Macedonia, in 1993 and the Ph.D. degree in electrical power engineering from Delft University of Technology, Delft, The Netherlands, in 2002. In 1997, he was an Academic Visitor with the University of Liverpool, working in the arc research group on modeling SF_6 circuit breakers. He is an Associate Professor in the Department of Electrical Sustainable Energy at the Delft University of Technology. His research interests include future power systems, large scale of power system transients, intelligent protection for future power systems, and wide area monitoring and protection. Dr. Popov received the prestigious Dutch Hidde Nijland award in 2010, the IEEE PES Prize Paper Award, and the IEEE Switchgear Committee Award in 2011. He is also an Associate Editor of *Elsevier's JEPES*. He is also a member of CIGRE and actively participated in Working Group C4.502 and Working Group A2/C4.39.

Lou van der Sluis (M'81–SM'86–LSM'16) was born in Geervliet, The Netherlands, in 1950. He received the M.Sc. degree in electrical engineering from the Delft University of Technology, Delft, The Netherlands, in 1974. He joined the KEMA High Power Laboratory in 1977 as a Test Engineer. In 1990, he became a part-time Professor and since 1992, he has been a full-time Professor in the Department of Power Systems, Delft University of Technology. He is the author of *Transients in Power Systems* and coauthor of *Electrical Power System Essentials* and *Switching in Electrical Transmission and Distribution Systems*. Prof. van der Sluis is a past convener of CC-03 of CIGRE and CIRED. He has been a member of CIGRE WG A3-24 on internal arc testing and a member of CIGRE WG C4-502 to study the interaction between high-voltage overhead lines and underground cables. He is a member of the advisory board of SC-A3 of CIGRE.

Jorrit A. Bos received the M.Sc. degree in electrical engineering from the Delft University of Technology, The Netherlands, in 2008. In 2008, he joined TenneT TSO as a Technical Trainee in the young professional program, where he worked in three different departments. Since 2010, he has been a Grid Strategist in the Department of Grid Development of TenneT. He currently holds the position of Senior Grid Strategist for the 150 kV grid developments in the southern part of the Netherlands. Next to that, his focus is on European grid development within the North Sea region, 380 kV cable research, and dynamic stability analysis.

Jan P. W. de Jong received the M.Sc. degree in electrical engineering from the Delft University of Technology, The Netherlands, in 2000. In 2001, he joined Transportnet Zuid Holland as a Grid Developer. Since 2004, he has worked at TenneT TSO as a Grid Strategist in the Grid Development Department. He currently holds the position of Senior Grid Strategist. Next to that, his focus is on the 380 kV cable research program in the Randstad area.

Akihiro Ametani (M'71–SM'83–F'92–LF'10) received the Ph.D. degree in power system transients from the Institute of Science and Technology (UMIST), University of Manchester, Manchester, U.K., in 1973, and the D.Sc. degree (higher degree in U.K.) from the University of Manchester, Manchester, U.K., in 2010. From 1971 to 1974, he was with the UMIST and Bonneville Power Administration, Portland, OR, USA, and developed an Electromagnetic Transients Program for Summers 1976 to 1981. Since 1985, he has been a Professor with Doshisha University, Kyoto, Japan, and was a Professor at the Chatholic University of Leaven, Leuven, Belgium, in 1988. He was the Director of the Institute of Science and Engineering from 1996 to 1998, and the Dean of Library and Computer/Information Center, Doshisha University, from 1998 to 2001. He was the Vice-President of the Institute of Electrical Engineers of Japan in 2003 and 2004. He is a Chartered Engineer in the U.K., a Fellow of IET, and a distinguished member of CIGRE.